Spin Manipulation in Graphene by Chemically Induced Pseudospin Polarization

Dinh Van Tuan[1,†] and Stephan Roche[1,2,*]
[1]Catalan Institute of Nanoscience and Nanotechnology (ICN2), CSIC and The Barcelona Institute of Science and Technology, Campus UAB, Bellaterra, 08193 Barcelona, Spain
[2]ICREA, Institució Catalana de Recerca i Estudis Avançats, 08070 Barcelona, Spain
(Received 19 November 2015; published 9 March 2016)

Spin manipulation is one of the most critical challenges to realize spin-based logic devices and spintronic circuits. Graphene has been heralded as an ideal material to achieve spin manipulation, but so far new paradigms and demonstrators are limited. Here we show that certain impurities such as fluorine adatoms, which locally break sublattice symmetry without the formation of strong magnetic moment, could result in a remarkable variability of spin transport characteristics. The impurity resonance level is found to be associated with a long-range sublattice pseudospin polarization, which by locally decoupling spin and pseudospin dynamics provokes a huge spin lifetime electron-hole asymmetry. In the dilute impurity limit, spin lifetimes could be tuned electrostatically from 100 ps to several nanoseconds, providing a protocol to chemically engineer an unprecedented spin device functionality.

DOI: 10.1103/PhysRevLett.116.106601

Introduction.—The possibility to fine-tune the electronic, charge, and spin transport properties of graphene using chemical functionalization [1–4], irradiation (defect formation) [5], electric fields [6], or antidot fabrication [7] has become an exciting field of research with almost endless possibilities. In particular, chemical treatments, such as ozonization, hydrogenation, or fluorination, introducing a variable density of surface adatoms from typically 0.001% to a few percent, have demonstrated a large spectrum of accessible physical states from anomalous transport to highly insulating behavior of chemically reactive graphene derivatives [8–12]. On the other hand, graphene exhibits long room temperature spin lifetime and rich surface chemistry opportunities that could be harnessed for the development of all-spin logic technologies [13–20]. As a matter of illustration, the use of chemical fluorination of graphene bilayer has been shown to yield very high spin injection efficiency (above 60%), owing to improved interface spin filtering [21].

Spin lifetime is an essential quantity that fixes the upper time and length scales on which spin devices can operate, so that knowing its value and variability are prerequisite to realizing graphene spintronic technologies. The sources of spin relaxation turn out to be diversified in graphene, and extrinsic disorder driven by adatom impurities can significantly enhanced spin-orbit interaction around defects [1] or create local magnetism [22], both effects usually reducing spin lifetimes, even in the dilute limit [23–31].

The nature of spin relaxation in graphene has been initially discussed either in terms of Elliot-Yafet (EY) [24] or Dyakonov-Perel (DP) [32] mechanisms, depending on the scaling of spin lifetime with defect density. However, recently, a novel spin relaxation mechanism in nonmagnetic graphene samples has been connected to the unique spin-pseudospin entanglement occurring near the Dirac point, pointing towards revisiting the role of sublattice pseudospin [33].

Sublattice pseudospin is an additional quantum degree of freedom, mathematically very similar to spin and unique to graphene sublattice degeneracy [1]. In the absence of spin-orbit coupling, the low-energy electronic states are $\Psi_{\vec{k}}(\vec{r}) \sim [\psi_A(1,0)^T + \psi_B(0,1)^T]e^{i\vec{k}\vec{r}}$, where $(1,0)^T$ and $(0,1)^T$ define up- and down-pseudospin states, while ψ_A (ψ_B) give the wave function weight restricted to A (B) sublattice sites [1,34]. In addition to sublattice pseudospin, valley isospin (for the two K points in the reciprocal space) also shows up in the electronic wave functions, and harnessing these degrees of freedom is the target of valleytronics and pseudospintronics [35,36]. The complex interplay between sublattice pseudospin and valley isospin is currently the source of innovative device proposals such as valley or pseudospin filtering and switches [6,37–42].

In the presence of a Rashba spin-orbit coupling (SOC) field generated by either a substrate-induced electric field or a weak density of metal adatoms (gold, nickel), spin and pseudospin become strongly coupled at the Dirac point where the eigenstates take the form $\Psi_{\vec{k}=\vec{K}} \sim (1,0)^T|\downarrow\rangle \pm i(0,1)^T|\uparrow\rangle$, where $|\downarrow\rangle$ and $|\uparrow\rangle$ denote the spin state [33,43]. Such spin-pseudospin locking drives to an entangled dynamics of spin and pseudospin resulting in fast spin dephasing, even when approaching the ballistic limit [33], with increasing spin lifetimes away from the Dirac point, as observed experimentally [44]. This phenomenon suggests ways to engineer spin manipulation based on controlling the pseudospin degree of freedom (or vice versa), which would help in the development of spin logics [16,19,20].

In this Letter, we reveal that chemical functionalization of graphene with certain types of adatoms such as fluorine, by breaking the sublattice symmetry and by inducing a SOC without the formation of strong magnetic moment, provides an enabling technique to monitor spin transport properties in a remarkable way for spintronic applications. The fluorine adatoms indeed produce hole impurity levels, which exhibit a long-range spatial sublattice pseudospin polarization (SPP), which counteracts the homogeneous Rashba SOC field at the origin of the intrinsic spin precession and relaxation in the otherwise fluorine-free samples [45]. As a result, spin and pseudospin dynamics are no longer coupled at the impurity resonances, which leads to the possibility to electrostatically tune spin lifetime by up to 1 order of magnitude (for instance, under electrostatic gating). This is a theoretical opportunity for designing a new kind of spin transistor effect based on a gate-controlled spin transport length. Calculations are performed using a realistic tight-binding model elaborated from *ab initio* calculations, whereas the spin dynamics is computed through the time evolution of the expectation value of the spin operator projected on a real-space basis set.

Tight-binding description of fluorinated graphene.—The description of fluorine adatom on graphene is achieved using a tight-binding model elaborated from *ab initio* simulations [47]. The Hamiltonian for the system involves two parts:

$$\mathcal{H} = \mathcal{H}_G + \mathcal{H}_{FG} \tag{1}$$

The first part describes the graphene in a homogeneous SOC field induced by the substrate or gate voltage,

$$\mathcal{H}_G = -\gamma_0 \sum_{\langle ij\rangle} c_i^+ c_j + \frac{2i}{9}\lambda_I \sum_{\langle\langle ij\rangle\rangle} c_i^+ \vec{s}\cdot(\vec{d}_{kj}\times\vec{d}_{ik})c_j + \frac{2i}{3}\lambda_R \sum_{\langle ij\rangle} c_i^+ \vec{z}\cdot(\vec{s}\times\vec{d}_{ij})c_j, \tag{2}$$

where γ_0 is the usual π-orbital hopping term between nearest neighbors, $\lambda_I = 12$ μeV is a common value used for the intrinsic SOC of graphene [49], while the Rashba SOC λ_R is an electric field-dependent quantity. In this study, we take $\lambda_R =$ 37.4 μeV taken from an extended sp-band tight-binding model [50] for graphene under the influence of an electric field of 0.1 V/Å, induced by the substrate or the gate voltage.

The second part, $\hat{\mathcal{H}}_{FG}$, describes the influences of fluorine on graphene

$$\hat{\mathcal{H}}_{FG} = \epsilon_F \sum_m F_m^+ F_m + T\sum_{\langle mi\rangle}[F_m^+ A_i + \text{H.c.}] + \frac{2i}{9}\Lambda_I^B \sum_{\langle\langle ij\rangle\rangle} B_i^+ \vec{s}.(\vec{d}_{kj}\times\vec{d}_{ik})B_j + \frac{2i}{3}\Lambda_R \sum_{\langle ij\rangle}[A_i^+ \vec{\hat{z}}.(\vec{s}\times\vec{d}_{ij})B_j + \text{H.c.}] + \frac{2i}{3}\Lambda_{\text{PIA}} \sum_{\langle\langle ij\rangle\rangle} B_i^+ \vec{\hat{z}}.(\vec{s}\times\vec{d}_{ij})B_j, \tag{3}$$

where all the parameters $\epsilon_F = -2.2$ eV, $T = 5.5$ eV, $\Lambda_I^B = 3.3$ meV, $\Lambda_R = 11.2$ meV, and $\Lambda_{PIA}^B = 7.3$ meV are derived from *ab initio* simulations [47]. The operator F (F^+) annihilates (creates) an electron in the atomic p_z orbital on fluorine F. A and B (A^+ and B^+) denote the annihilation (creation) operators for the p_z orbital on fluorinated carbons and their nearest neighbors, respectively. The first term in the above Hamiltonian is the on-site energy term on the fluorine adatoms, and the second term is the hopping term between fluorine adatoms F and fluorinated carbon $A \equiv C_F$. The third and fourth terms, which are similar to the SOC terms in Eq. (2), simulate the local intrinsic and Rashba SOCs induced by the absorption of fluorine on graphene. Finally, the last term, the new SOC term, coming from the pseudospin inversion asymmetry (PIA) mediates the spin-flip hopping between two second-nearest neighbors B_i. It is worth mentioning that we are using the π-orbital tight-binding model, which is different from a recent Letter on the electronic structures and optical properties of fluorinated graphene in which the multiorbital tight-binding was employed [51].

Spin dynamics methodology.—The spin dynamics of electron in fluorinated graphene is investigated using the time-dependent evolution of the spin polarization of propagating wave packets [33]. Simulations of samples of μm^2 size are performed, containing hundreds of millions of carbon atoms ($N \sim 10^8$). The time evolution of the spin polarization is computed through

$$\vec{P}(E,t) = \frac{\langle\Psi(t)|\vec{s}\delta(E-\mathcal{H}) + \delta(E-\mathcal{H})\vec{s}|\Psi(t)\rangle}{2\langle\Psi(t)|\delta(E-\mathcal{H})|\Psi(t)\rangle}, \tag{4}$$

where $\vec{s}$ are the spin Pauli matrices and $\delta(E-\mathcal{H})$ is the spectral measure operator. The time evolution of electronic wave packets $|\Psi(t)\rangle$ is obtained by solving the Schrödinger equation [52,53], starting from random-phase states $|\Psi(t=0)\rangle = |\varphi_{\text{RP}}\rangle$ with an initial out-of-plane (z direction) or in-plane polarization (x, y direction). The random-phase states can be generally expressed as

$$|\varphi_{\text{RP}}\rangle = \frac{1}{\sqrt{N}}\sum_{j=1}^{N}\begin{pmatrix}\cos(\theta_j/2)\\ e^{i\Phi_j}\sin(\theta_j/2)\end{pmatrix} e^{2i\pi\alpha_j}|j\rangle,$$

where (Φ_j, θ_j) gives the spin orientation of the orbital $|j\rangle$ in the spherical coordinate, whereas α_j is a random number in the [0, 1] interval [33]. An energy broadening parameter η is introduced for expanding $\delta(E-\mathcal{H})$ through a continued fraction expansion of the Green function [52,53]. An average over a few tens of random-phase states is usually sufficient to converge the expectation values. This method has been previously used to investigate spin relaxation in gold-decorated graphene [33], hydrogenated graphene [26], and, recently, SOC coupled graphene under the effect of electron-hole puddles [45,46].

Impurity resonance and sublattice pseudospin polarization.—Electronic calculations show that, unlike hydrogen, the fluorine adatom is a broad scatterer [47]. The DOS of a 40×40 supercell (about 0.03%) exhibits a resonant peak at about 260 meV [47] below the Dirac point. Figure 1 shows the LDOS on the sites close to the fluorinated carbon C_F using the tight-binding model for $\mathcal{H}$ [Eq. (1)]. All the LDOSs present a strong electron-hole asymmetry with broad peaks at about $E_R = -0.125\gamma_0 = -325$ meV, which are evidences of fluorine-induced resonant effect. More interestingly, the height of resonant peaks discloses a sublattice asymmetry with less state occupancy on the sublattice related to the fluorinated carbon C_F. This is the signature of a SPP, which is present in graphene when the A-B symmetry is broken, such as in the case of hydrogenated, nitrogen-doped graphene, or (bi)-graphene with vacancies [48]. Fluorine adatoms induce a long-range pseudospin-polarized region. Figure 1 (inset) shows the LDOS at the resonant energy E_R (represented by the radius of circles) on more than 300 atoms around the fluorinated carbon (marked by the green dot). At the edge of this area one can still see the difference between LDOSs on two different sublattices. Here we will show that the SPP has a direct impact on the spin lifetime in fluorinated graphene.

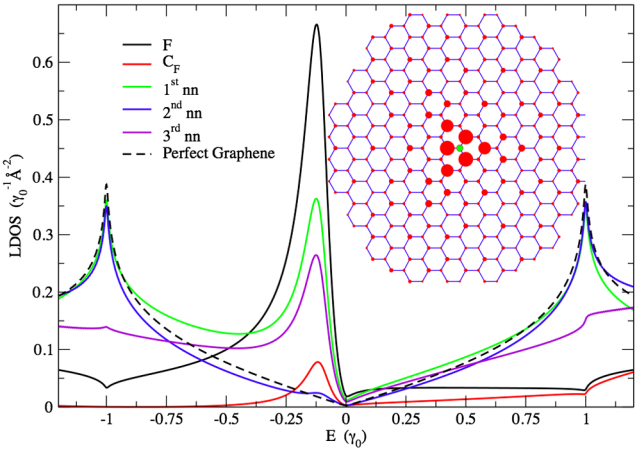

FIG. 1. Local density of states (solid lines) around the fluorinated carbon C_F in comparison with the pristine graphene one (dashed line). Inset: SPP around the fluorinated carbon (marked by the green circle). The radii of the circles are proportional to the LDOS; the state is projected at the resonant energy $E_R = -0.125\gamma_0$.

Strong electron-hole asymmetry of the spin lifetime.—We compute the expectation value of the out-of-plane spin component $P_z(E,t) = P_\perp(E,t)$ and the in-plane spin component $P_x(E,t) = P_\parallel(E,t)$ of spin polarization in fluorinated graphene using Eq. (4). Figure 2(c) (inset) shows the evolution of spin polarization $P_z(t)$ at the Dirac point (black and green solid lines) and at the resonant energies E_R (red and blue solid lines) for 0.01% and 0.02% of fluorine on graphene. There are two interesting features of the spin signals. The first one is the remarkably slow decay of the time evolution of the spin polarization at the resonance ($E = E_R$) compared to that occurring at the Dirac point. The second characteristic is the enhancement of spin polarization when increasing the percentage of fluorine [see illustration in Figs. 2(a) and 2(b)].

Such remarkable features are further manifested in the spin lifetime τ_s [Fig. 2(c), main frame], which are extracted from the spin polarization by fitting the obtained data with an exponential decay $P_{x,z}(t) = P_{x,z}(t_0)e^{-(t-t_0)/\tau_s^{\parallel,\perp}}$ [dashed lines in the inset of Fig. 2(c)]. This fitting is performed starting from the time $t_0 = 30$ ps to avoid the initially transient fast decay that is usually observed for strong disorder, especially at DP [26]. The spin lifetime exhibits a strong electron-hole asymmetry with a huge increase of

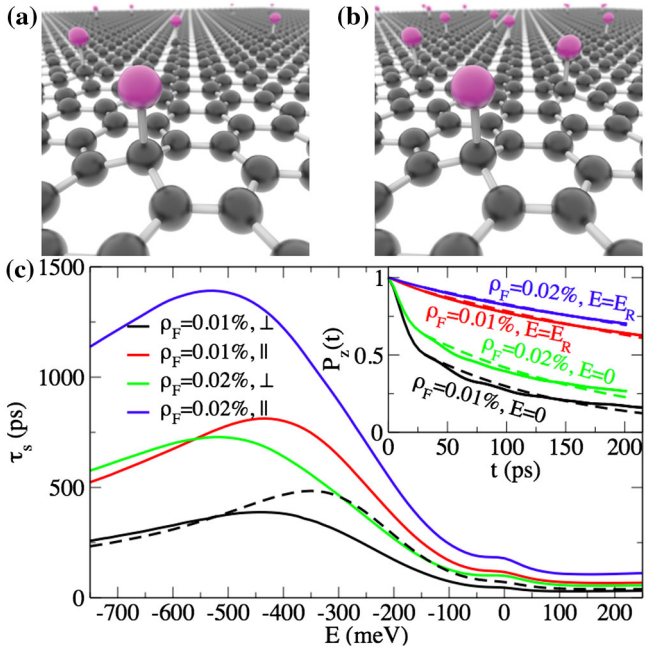

FIG. 2. (a),(b) Ball-and-stick models for fluorine functionalized graphene for two different densities. (c) Spin relaxation time τ_s for in-plane ($\parallel$) and out-of-plane ($\perp$) spin components for 0.01% and 0.02% of fluorine on graphene (dashed line gives $\tau_s^\perp$ for 0.01% fluorine, neglecting the SOC terms induced by fluorine). Inset: Spin polarization evolution at the Dirac point and at resonant energy E_R for 0.01% and 0.02% of fluorine on graphene.

spin lifetime with a maximum close to but not exactly at the resonant energy (about 1 order of magnitude compared to one in the electron side).

The energy of this maximum is shifted to the hole side compared to the resonant energy E_R and this energy shift increases with the fluorine concentration. This shift is attributed to the SOC effects caused by fluorine adatoms. Indeed, turning off the SOC induced by fluorine leads to the spin lifetime (dashed line) with the peak exactly at resonant energy E_R. More remarkably, the increase of fluorine percentage leads to an enhancement of τ_s [Fig. 2(c)]. This is counterintuitive because fluorine was predicted to induce a giant SOC in graphene, which should lead to a decrease of spin lifetime with fluorine density ρ_F [47]. Actually, the SOC induced by fluorine does not play a major role here. Indeed, in the absence of SOC induced by fluorine ($\Lambda_I^B = \Lambda_R = \Lambda_{\mathrm{PIA}} = 0$), τ_s shows similar energy dependence [see dashed line in Fig. 2(c) for $\tau_s^\perp$ and 0.01% fluorine atoms neglecting their SOC contribution].

Dyakonov-Perel mechanism.—Fluorine adatoms also induce momentum scattering, which yields randomization of the spin precession. This usually leads to a DP relaxation mechanism in which the spin lifetime τ_s is inversely proportional to the momentum relaxation time τ_p; i.e., $\tau_s^\parallel = 2\tau_s^\perp = \hbar^2/(2\lambda_R^2\tau_p)$ [32,54–56]. This scaling can be clearly observed in Fig. 2(c), where τ_s upscales with the fluorine density ρ_F almost linearly, as expected from a Fermi golden rule argument. To further confirm the mechanism at play, the momentum relaxation time τ_p is computed numerically using a real-space order-N approach [53].

Figure 3(a) shows the energy dependence of τ_p for 0.02% of fluorine on graphene with a minimum close to E_R, pinpointing the resonance induced by fluorine (identified by the peak in the LDOS; see red dashed line). To further confirm the relaxation mechanism, we compute the product of $\tau_s\tau_p$ [see Fig. 3(b)]. The obtained numerical data (black solid line) close to the resonance are fairly consistent with a DP mechanism (red dashed line) up to a factor $\alpha \in [0.6; 1.4]$ [$\tau_s^\parallel\tau_p = (\alpha\hbar^2/2\lambda_R^2)$]. A final evidence is given by the spin lifetime anisotropy of τ_s obtained in Fig. 3(c). Indeed, the ratio of in-plane and out-of-plane spin lifetimes $\tau_s^\parallel/\tau_s^\perp \sim 2$ (within 10% error) well agrees with analytical calculations performed in model systems [56]. Some deviation is observed close to the Dirac point, where the spin-pseudospin entanglement effects are maximized.

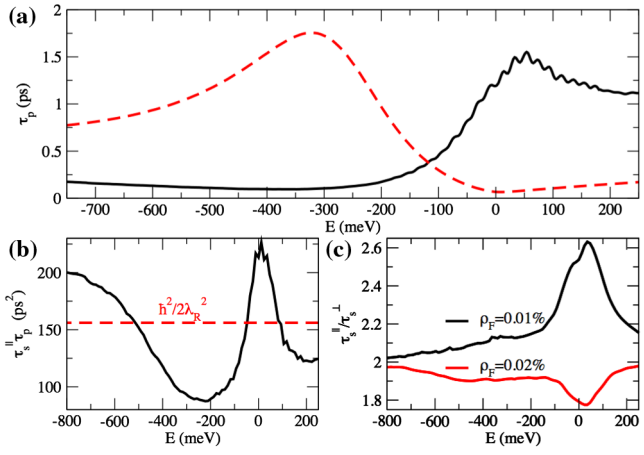

FIG. 3. (a) Energy dependence of the momentum relaxation time τ_p for 0.02% of fluorine on graphene. (b) Numerical product of $\tau_s^\parallel\tau_p$ compared with the analytical value (dashed line) from Ref. [32]. (c) The ratio of in-plane and out-of-plane spin relaxation times for 0.01% and 0.02% of fluorine on graphene.

Discussion.—The enhancement and the energy dependence of τ_s are a direct consequence of defect-induced sublattice pseudospin polarization (illustrated in Fig. 1, inset). In supported ultraclean graphene, the Rashba SOC λ_R induced by the substrate or the gate voltage dictates the spin dephasing of propagating charges, as shown experimentally [44]. It is worth mentioning that the spin lifetime caused by this background Rashba SOC is totally electron-hole symmetric [45]. On the hole side, the induced SPP around fluorine defects locally suppress the Rashba SOC and consequently enhance spin lifetime up to the range of nanoseconds, whereas τ_s is more strongly reduced on the electron side, with $\tau_s \sim 100$ ps. This phenomenon can be qualitatively understood using both the continuum and tight-binding models. In the continuum model, the Hamiltonian $\mathcal{H}_G$ [Eq. (2)], including spin-orbit interaction, can be approximated as $h_G(\vec{k}) = \hbar v_F(\eta\sigma_x k_x + \sigma_y k_y) + \lambda_R(\eta\sigma_x s_y - \sigma_y s_x) + \lambda_I\eta\sigma_z s_z$, where σ and s are Pauli matrices representing the sublattice pseudospin and spin degrees of freedom, respectively, while $\eta = 1(-1)$ corresponds to the K (K') valley (here, intervalley coupling is neglected in the discussion). The magnitude of the Rashba magnetic field is proportional to the in-plane component of pseudospin (σ_x, σ_y) [33], which is reduced by approaching the area around fluorine due to the formation of SPP. The reduction of the local effective Rashba magnetic field entails the enhancement of spin lifetimes, which is maximum close to the resonant energy E_R where the SPP is maximum. In the tight-binding model, the peculiar sublattice occupancy of impurity states gives rise to an increase of the next-nearest-neighbor hopping probability (intrinsic SOC) and a decrease of the nearest-neighbor hopping probability (Rashba SOC), which being the main factor for spin relaxation also explains the spin lifetime enhancement.

One notes that SPP is not unique to fluorine adsorption in the weak density limit, but can also be generated by nitrogen substitutions [57], grafted molecules [58], hydrogen adatoms, or any other effect breaking A-B sublattice symmetry. However, the unveiled phenomenon of electron-hole spin transport asymmetry should be maximized in the absence of magnetic moments, which disfavor long spin propagation [25,26]. Additionally, in contrast to the EY mechanism predicted for magnetic impurities [25,26,30],

adatoms such as fluorine are shown here to entail a DP mechanism, in agreement with many experiments on functionalized graphene [59,60]. We note that the considered dilute fluorine limit is accessible experimentally [61,62], and that chemical bonding of fluorine adatoms is theoretically tunable with electric field [63–65], a fact that could help in controlling the level of adsorption and the possibility to switch on and off the spin transport asymmetry generated by impurities. Finally, we observe that spin dynamics could be a smoking gun for unveiling a new quantum phase transition resulting from the competition between different ground states (such as those characterized by spin-degenerate and magnetic bound states [66]), or to scrutinize the origin of the saturation of coherence times in weak localization measurements [67].

This work has received funding from the European Union Seventh Framework Programme under Grant Agreement No. 604391 Graphene Flagship. S. R. acknowledges the Spanish Ministry of Economy and Competitiveness for funding (MAT2012-33911), the Secretaria de Universidades e Investigacion del Departamento de Economia y Conocimiento de la Generalidad de Cataluña, and the Severo Ochoa Program (MINECO SEV-2013-0295).

*stephan.roche@icn.cat
†Present address: Department of Electrical and Computer Engineering, University of Rochester, Rochester, NY 14627, USA.

[1] A. H. Castro Neto, F. Guinea, N. M. R. Peres, K. S. Novoselov, and A. K. Geim, Rev. Mod. Phys. **81**, 109 (2009).
[2] A. V. Krasheninnikov and F. Banhart, Nat. Mater. **6**, 723 (2007).
[3] K. P. Loh, Q. Bao, P. K. Ang, and J. Yang, J. Mater. Chem. **20**, 2277 (2010).
[4] M. F. Craciun, I. Khrapach, M. D. Barnes, and S. Russo, J. Phys. Condens. Matter **25**, 423201 (2013).
[5] R. R. Nair, M. Sepioni, I.-L. Tsai, O. Lehtinen, J. Keinonen, A. V. Krasheninnikov, T. Thomson, A. K. Geim, and I. V. Grigorieva, Nat. Phys. **8**, 199 (2012).
[6] Y. Son, L. Cohen, and S. Louie, Nature (London) **444**, 347 (2006).
[7] T. G. Pedersen, C. Flindt, J. Pedersen, N. A. Mortensen, A.-P. Jauho, and K. Pedersen, Phys. Rev. Lett. **100**, 136804 (2008).
[8] D. Elias, R. Nair, T. Mohiuddin, S. Morozov, P. Blake, M. Halsall, A. Ferrari, D. Boukhvalov, M. Katsnelson, A. Geim, and K. Novoselov, Science **323**, 610 (2009).
[9] F. Withers, M. Dubois, and A. K. Savchenko, Phys. Rev. B **82**, 073403 (2010).
[10] J. Moser, H. Tao, S. Roche, F. Alsina, C. M. Sotomayor Torres, and A. Bachtold, Phys. Rev. B **81**, 205445 (2010).
[11] S.-H. Cheng, K. Zou, F. Okino, H. R. Gutierrez, A. Gupta, N. Shen, P. C. Eklund, J. O. Sofo, and J. Zhu, Phys. Rev. B **81**, 205435 (2010).
[12] J. T. Robinson, J. S. Burgess, C. E. Junkermeier, S. C. Badescu, T. L. Reinecke, F. K. Perkins, M. K. Zalalutdniov, J. W. Baldwin, J. C. Culbertson, P. E. Sheehan, and E. S. Snow, Nano Lett. **10**, 3001 (2010).
[13] N. Tombros, C. Jozsa, M. Popinciuc, H. Jonkman, and B. Van Wees, Nature (London) **448**, 571 (2007).
[14] B. Dlubak, M.-B. Martin, C. Deranlot, B. Servet, S. Xavier, R. Mattana, M. Sprinkle, C. Berger, W. de Heer, F. Petroff, A. Anane, P. Seneor, and A. Fert, Nat. Phys. **8**, 557 (2012).
[15] P. Seneor, B. Dlubak, M. Martin, A. Anane, H. Jaffres, and A. Fert, MRS Bull. **37**, 1245 (2012).
[16] H. Dery, H. Wu, B. Ciftcioglu, M. Huang, Y. Song, R. Kawakami, J. Shi, I. Krivorotov, I. Zutic, and L. J. Sham, IEEE Trans. Electron Devices **59**, 259 (2012).
[17] M. B. Lundeberg, R. Yang, J. Renard, and J. A. Folk, Phys. Rev. Lett. **110**, 156601 (2013).
[18] M. Venkata Kamalakar, C. Groenveld, A. Dankert, and S. Dash, Nat. Commun. **6**, 6766 (2015).
[19] R. K. Kawakami, 2D Mater. **2**, 034001 (2015).
[20] S. Roche, J. Akerman, B. Beschoten, J.-C. Charlier, M. Chshiev, S. P. Dash, B. Dlubak, J. Fabian, A. Fert, M. Guimares, F. Guinea, I. Grigorieva, C. Schnenberger, P. Seneor, C. Stampfer, S. O. Valenzuela, X. Waintal, and B. van Wees, 2D Mater. **2**, 030202 (2015).
[21] A. Friedman, O. vant Erve, C. Li, J. Robinson, and B. Jonker, Nat. Commun. **5**, 3161 (2014).
[22] O. V. Yazyev, Phys. Rev. Lett. **101**, 037203 (2008).
[23] D. Huertas-Hernando, F. Guinea, and A. Brataas, Phys. Rev. Lett. **103**, 146801 (2009).
[24] H. Ochoa, A. H. Castro Neto, and F. Guinea, Phys. Rev. Lett. **108**, 206808 (2012).
[25] D. Kochan, M. Gmitra, and J. Fabian, Phys. Rev. Lett. **112**, 116602 (2014).
[26] D. Soriano, D. V. Tuan, S. M.-M. Dubois, M. Gmitra, A. W. Cummings, D. Kochan, F. Ortmann, J.-C. Charlier, J. Fabian, and S. Roche, 2D Mater. **2**, 022002 (2015).
[27] D. Kochan, S. Irmer, M. Gmitra, and J. Fabian, Phys. Rev. Lett. **115**, 196601 (2015).
[28] S. Omar, M. Gurram, I. J. Vera-Marun, X. Zhang, E. H. Huisman, A. Kaverzin, B. L. Feringa, and B. J. van Wees, Phys. Rev. B **92**, 115442 (2015).
[29] M. R. Thomsen, M. M. Ervasti, A. Harju, and T. G. Pedersen, Phys. Rev. B **92**, 195408 (2015).
[30] J. Bundesmann, D. Kochan, F. Tkatschenko, J. Fabian, and K. Richter, Phys. Rev. B **92**, 081403 (2015).
[31] S. Lara-Avila, S. Kubatkin, O. Kashuba, J. A. Folk, S. Lüscher, R. Yakimova, T. J. B. M. Janssen, A. Tzalenchuk, and V. Fal'ko, Phys. Rev. Lett. **115**, 106602 (2015).
[32] C. Ertler, S. Konschuh, M. Gmitra, and J. Fabian, Phys. Rev. B **80**, 041405 (2009).
[33] D. Van Tuan, F. Ortmann, D. Soriano, S. Valenzuela, and S. Roche, Nat. Phys. **10**, 857 (2014).
[34] Y. Liu, G. Bian, T. Miller, and T.-C. Chiang, Phys. Rev. Lett. **107**, 166803 (2011).
[35] D. Pesin and A. H. MacDonald, Nat. Mater. **11**, 409 (2012).
[36] U. Zuelicke, in *Optoelectronic and Microelectronic Materials & Devices (COMMAD), 2014 Conference on, Perth, WA* (2014), pp. 54–55.

[37] A. Rycerz, J. Tworzydlo, and C. Beenakker, Nat. Phys. **3**, 172 (2007).
[38] P. San-Jose, E. Prada, E. McCann, and H. Schomerus, Phys. Rev. Lett. **102**, 247204 (2009).
[39] G. Tkachov and M. Hentschel, Phys. Rev. B **79**, 195422 (2009).
[40] C. Park, H. Yang, A. J. Mayne, G. Dujardin, S. Seo, Y. Kuk, J. Ihm, and G. Kim, PNAS **108**, 18622 (2011).
[41] D. Gunlycke and C. T. White, Phys. Rev. Lett. **106**, 136806 (2011).
[42] M. B. Lundeberg and J. A. Folk, Science **346**, 422 (2014).
[43] E. I. Rashba, Phys. Rev. B **79**, 161409 (2009).
[44] M. H. D. Guimarães, P. J. Zomer, J. Ingla-Aynés, J. C. Brant, N. Tombros, and B. J. van Wees, Phys. Rev. Lett. **113**, 086602 (2014).
[45] D. Van Tuan, F. Ortmann, A. Cummings, D. Soriano, and S. Roche, Sci. Rep. **6**, 21046 (2015).
[46] A. W. Cummings and S. Roche, Phys. Rev. Lett. **116**, 086602 (2016).
[47] S. Irmer, T. Frank, S. Putz, M. Gmitra, D. Kochan, and J. Fabian, Phys. Rev. B **91**, 115141 (2015).
[48] D. V. Tuan and S. Roche, Phys. Rev. B **93**, 041403(R) (2016).
[49] M. Gmitra, S. Konschuh, C. Ertler, C. Ambrosch-Draxl, and J. Fabian, Phys. Rev. B **80**, 235431 (2009).
[50] C. R. Ast and I. Gierz, Phys. Rev. B **86**, 085105 (2012).
[51] S. Yuan, M. Rösner, A. Schulz, T. O. Wehling, and M. I. Katsnelson, Phys. Rev. Lett. **114**, 047403 (2015).
[52] S. Roche and D. Mayou, Phys. Rev. Lett. **79**, 2518 (1997).
[53] S. Roche, Phys. Rev. B **59**, 2284 (1999).
[54] M. I. Dyakonov and V. I. Perel, Sov. Phys. Solid State **13**, 3023 (1972).
[55] D. Huertas-Hernando, F. Guinea, and A. Brataas, Phys. Rev. Lett. **103**, 146801 (2009).
[56] P. Zhang and M. W. Wu, New J. Phys. **14**, 033015 (2012).
[57] L. Zhao, R. He, K. T. Rim, T. Schiros, K. S. Kim, H. Zhou, C. Gutiérrez, S. P. Chockalingam, C. J. Arguello, L. Pálová, D. Nordlund, M. S. Hybertsen, D. R. Reichman, T. F. Heinz, P. Kim, A. Pinczuk, G. W. Flynn, and A. N. Pasupathy, Science **333**, 999 (2011).
[58] K. S. Mali, J. Greenwood, J. Adisoejoso, R. Phillipson, and S. De Feyter, Nanoscale **7**, 1566 (2015).
[59] M. Wojtaszek, I. J. Vera-Marun, T. Maassen, and B. J. van Wees, Phys. Rev. B **87**, 081402 (2013).
[60] A. G. Swartz, K. M. McCreary, W. Han, J. J. I. Wong, P. M. Odenthal, H. Wen, J.-R. Chen, R. K. Kawakami, Y. Hao, R. S. Ruoff, and J. Fabian, J. Vac. Sci. Technol. B **31**, 105 (2013).
[61] X. Hong, S.-H. Cheng, C. Herding, and J. Zhu, Phys. Rev. B **83**, 085410 (2011).
[62] A. Avsar, J. Hak Lee, G. K. Wai Koon, and B. Özyilmaz, 2D Mater. **2**, 044009 (2015).
[63] J. O. Sofo, A. M. Suarez, G. Usaj, P. S. Cornaglia, A. D. Hernández-Nieves, and C. A. Balseiro, Phys. Rev. B **83**, 081411 (2011).
[64] M. Guzman-Arellano, A. D. Hernandez-Nieves, C. A. Balseiro, and G. Usaj, Appl. Phys. Lett. **105**, 121606 (2014).
[65] R. M. Guzmán-Arellano, A. D. Hernández-Nieves, C. A. Balseiro, and G. Usaj, Phys. Rev. B **91**, 195408 (2015).
[66] L. H. Guessi, Y. Marques, R. S. Machado, K. Kristinsson, L. S. Ricco, I. A. Shelykh, M. S. Figueira, M. de Souza, and A. C. Seridonio, Phys. Rev. B **92**, 245107 (2015).
[67] X. Hong, K. Zou, B. Wang, S.-H. Cheng, and J. Zhu, Phys. Rev. Lett. **108**, 226602 (2012).